ISSN 1063-7761, Journal of Experimental and Theoretical Physics, 2013, Vol. 117, No. 3, pp. 439–448. © Pleiades Publishing, Inc., 2013.

Two Regimes of Vortex Penetration into Platelet-Shaped Type-II Superconductors[1]

E. H. Brandt[a†], G. P. Mikitik[b], and E. Zeldov[c]

[a] *Max-Planck-Institut für Metallforschung, Stuttgart, D-70506 Germany*

[b] *Verkin Institute for Low Temperature Physics & Engineering, Ukrainian Academy of Sciences, Kharkov, 61103 Ukraine*

[c] *Department of Condensed Matter Physics, Weizmann Institute of Science, Rehovot, 76100 Israel*

e-mail: mikitik@ilt.kharkov.ua

Received March 26, 2013

Dedicated to the memory of Professor Anatoly Larkin

Abstract—Vortex penetration into a thin superconducting strip of a rectangular cross section is considered at an increasing applied magnetic field H_a, taking an interplay between the Bean–Livingston and the geometric barriers in the sample into account. We calculate the magnetic field H_p at which the penetration begins and show that two regimes of vortex penetration are possible. In the first regime, vortices appearing at the corners of the strip at $H_a = H_p$ immediately move to its center, where a vortex dome starts to develop. In the second regime, the penetration occurs in two stages. In the first stage, at $H_a < H_p$, tilted vortices penetrate into the edge regions of the strip, where novel domes are shown to be formed at the top, bottom, and lateral surfaces. In the second stage, at $H_a = H_p$, the vortex propagation to the center becomes possible. The difference between the regimes manifests itself in slightly different dependences of the magnetic moment of the strip on H_a.

DOI: 10.1134/S1063776113110010

1. INTRODUCTION

The Bean–Livingston [1] and geometric [2] barriers are important for understanding many phenomena in type-II superconductors. In particular, these barriers lead to a hysteretic magnetic behavior of the superconductors even in the absence of any bulk pinning of vortices [1–7]. Both these barriers also influence the magnetic relaxation [8, 9] and transport properties of superconductors [10–13]. Various manifestations of the Bean–Livingston and geometric barriers were experimentally studied in numerous works [14–31]. In this paper, we theoretically consider how an interplay between the geometric and Bean–Livingston barriers influences the vortex penetration into a platelet-shaped type-II superconductor placed in a perpendicular magnetic field H_a. For simplicity, we assume that flux-line pinning is negligible in the superconductor.

The Bean–Livingston barrier in bulk superconductors is due to the attraction of a penetrating vortex to the sample surface at distances of the order of the London penetration depth λ [1]. In the increasing magnetic field H_a, the attraction leads to a delay of the vortex penetration compared to the lower critical field H_{c1}. As a result, the penetration is possible only at the field H_p that can reach [32] $\kappa H_{c1}/\ln\kappa$, the thermodynamic critical field, where $\kappa = \lambda/\xi$ is the Ginzburg–Landau parameter and ξ is the coherence length.

The geometric barrier has a different origin and is due to the shape of the superconductor [2, 16]. This barrier appears for samples different from an ellipsoid. In an ellipsoid–shaped superconductor at the magnetic field $H_{\rm eq} = (1 - N)H_{c1}$, the self-energy $e_0 l(\mathbf{r})$ of a straight vortex placed at any point $\mathbf{r}$ of the sample is exactly equal to the work $W(\mathbf{r}, H_{\rm eq})$ done by the Meissner currents circulating in the sample to transfer the vortex from the surface of the superconductor to this point. Here, $e_0 = (\Phi_0/4\pi\lambda)^2\ln(\lambda/\xi)$ is the vortex energy per unit length, Φ_0 is the flux quantum, $l(\mathbf{r})$ is the length of the vortex passing through the point $\mathbf{r}$, and N is the appropriate demagnetizing factor of the ellipsoid. This specific property of the ellipsoid-shaped superconductors leads to the penetration of vortices into the sample just at the equilibrium penetration magnetic field $H_{\rm eq}$ (if the vortex attraction to the surface is neglected). In the platelet-shaped superconductors, the position-dependent energy of a vortex,

$$E(\mathbf{r}, H_a) = e_0 l(\mathbf{r}) - W(\mathbf{r}, H_a),$$

sharply increases near the edges due to the increase in the vortex length l from zero to the sample thickness d and decreases toward the center of the platelet due to the effect of the Meissner currents. This geometric barrier prevents the vortex penetration into the sample

† Deceased.

[1] The article is published in the original.

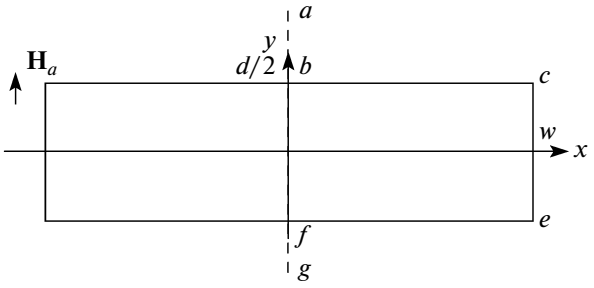

Fig. 1. The magnetic field line (a–b–c–e–f–g) adjoining a superconducting strip in the Meissner state. Under the conformal map described in the text, this line is the image of the real axis of the complex plane.

at the field H_{eq} that can now be defined as the lowest field at which the minimum of $e_0 d - W(\mathbf{r}, H_{eq})$ with respect to $\mathbf{r}$ reaches zero. Vortex penetration begins only at a higher field $H_a = H_p$ when the barrier near the edges disappears. At $H_a > H_p$, the penetrating vortices are accumulated in the region of the superconductor where $E(\mathbf{r})$ has a minimum with respect to $\mathbf{r}$, and hence a vortex dome appears near the center of the platelet.

Two situations may occur for the platelet-shaped superconductors. In the case of thin superconducting films whose thickness d is essentially less than the London penetration depth λ, the attraction of a vortex to the film edges develops on the scale noticeably larger than the effective penetration depth $\lambda_{eff} = \lambda^2/d \gg \lambda$, d [33], whereas the effect of the vortex-length variation is not essential in this case. This situation of the extended Bean–Livingston barrier can be described by replacing $e_0 l$ in $E(\mathbf{r})$ with an appropriate attraction potential $U_{attr}(\mathbf{r})$, and the process of vortex penetration into such films reveals features [10, 34] that are similar to the features in the case of a purely geometrical barrier [2]. In the second case of bulk platelet-shaped superconductors, we have $\lambda \ll d$, and the vortex attraction to the surface is essential only at distances of the order of λ, whereas the geometrical barrier develops on the scale of the order of d. Just this case $\lambda \ll d$ is studied in our paper.

In this paper, we consider a thin superconducting strip of a rectangular cross section of width $2w$ ($-w \le x \le w$) and thickness d ($-d/2 \le y \le d/2$; $d \ll w$), which infinitely extends in the z direction. The magnetic field is directed along the y axis. In this case, we have [2]

$$H_{eq} = (d/2w)H_{c1}, \quad H_p \sim H_{c1}\sqrt{d/w} \gg H_{eq}.$$

This estimate of H_p is based on formulas for the Meissner currents circulating in an infinitely thin strip [35] and on cutting off these currents in the edge region $w - d \lesssim |x| \le w$, where they diverge. However, such an approach cannot give an accurate result for the currents in this edge region, which is especially important for the understanding of the geometric and Bean–Livingston barriers in the strip. To investigate both these barriers in more detail and the interplay between them, we cannot neglect the thickness of the strip, and in this paper we find a two-dimensional distribution of the currents in the xy plane of the strip. For simplicity, we assume below that the superconductor is isotropic and that the applied field H_a is not too large, and hence the magnetic induction B in the sample is noticeably less than the low critical field H_{c1}. This assumption on B simplifies our analysis of the geometric barrier.

The paper is structured as follows. In Section 2, we present a two-dimensional distribution of the Meissner currents in a thin strip with a rectangular cross section. Using this distribution, the magnetic fields of the vortex penetration through the Bean–Livingston barrier in a corner of the strip and through the geometric barrier are estimated in Section 3, and it is shown that two regimes of vortex penetration into the sample can occur depending on the relation between these fields. In Section 4, the penetration field due to the geometric barrier is analyzed with a consideration of stray fields of the penetrating vortices. In Sections 5 and 6, we discuss and briefly summarize the obtained results. Some mathematical details are presented in the Appendix.

2. MEISSNER STATE IN A THIN STRIP WITH RECTANGULAR CROSS SECTION

For the strip in the Meissner state, the magnetic field $\mathbf{H}(x, y)$ outside the sample can be found from the Maxwell equations

$$\mathrm{div}\mathbf{H} = 0, \quad \mathrm{curl}\mathbf{H} = 0,$$

and hence the field can be described both by the scalar potential

$$\varphi(x, y), \quad \mathbf{H} = -\nabla\varphi,$$

and by the vector potential

$$\mathbf{A} = \mathbf{z}A(x, y), \quad \mathbf{H} = \mathrm{curl}\mathbf{A},$$

where $\mathbf{z}$ is the unit vector along the z axis. The complex potential $\varphi - iA$ is known [36] to be an analytic function of $x + iy$. For the strip with a rectangular cross section, this potential can be obtained using a conformal map of the upper half of the complex plane to the region lying to the right of the line a–b–c–e–f–g in Fig. 1 (the a–b–c–e–f–g contour coincides with the magnetic field line $A = 0$). This region is a rectangle with one of its sides passing through the infinite point, and the map can be found using the Schwarz–Christoffel formula [37]. In the map, the upper surface of the strip (the segment b–c), its lateral surface c–e, and its lower surface e–f are parameterized by a single variable t. This variable t ranges from $-1/\sqrt{m}$ (point b) to $1/\sqrt{m}$ (point f), where m is a constant parameter, $0 \le m \le 1$, whose value is determined by d/w. At the corners of the strip, we have $t = \pm 1$, and $t = 0$ at the point $x = w$, $y = 0$. Calculating $\mathbf{H} = -\nabla\varphi$ using the obtained

potential at the surface of the strip (**H** is tangential to the surface), we find the Meissner sheet currents $J_z = J$ flowing on the strip surface because we have $|J| = (c/4\pi)|\mathbf{H}|$ for any surface point.

These Meissner currents in the strip with an arbitrary ratio d/w were found previously [38] under the only assumption that $\lambda \ll d, w$. Here, we present the appropriate formulas in the case of a thin strip, when $d \ll w$. In this limit case, we arrive at the following parametric representations for the lateral surface $x = w$ of the strip:

$$\frac{y}{d} \approx -\frac{1}{\pi}(\arcsin(t) + t\sqrt{1-t^2}), \tag{1}$$

where $-1 \le t \le 1$, whereas for the upper ($-1/\sqrt{m} \le t \le -1$) and lower ($1 \le t \le 1/\sqrt{m}$) surfaces of the strip, we have:

$$\frac{w-x}{w} = \frac{f_1(|t|, m)}{f_1(1/\sqrt{m}, m)}, \tag{2}$$

where

$$f_1(|t|, m) = m\int_1^{|t|} \frac{\sqrt{s^2-1}}{\sqrt{1-ms^2}}ds,$$

$m \approx 2d/\pi w \ll 1$, and $f_1(1/\sqrt{m}, m) \approx 1$. The Meissner surface currents on all these surfaces are described by the unified formula

$$\frac{4\pi J(t)}{cH_a} = \frac{\sqrt{1-mt^2}}{\sqrt{m}\sqrt{|1-t^2|}}, \tag{3}$$

where $|t| \le 1/\sqrt{m}$.

At $t^2 \gg 1$, i.e., at $w - x \gg d$, we find from Eq. (2) that $x/w \approx \sqrt{1-mt^2}$, and with Eq. (3), we arrive at the well-known result obtained in the limit of the infinitely thin strip [2, 35]:

$$J\left(x, \frac{d}{2}\right) = J\left(x, -\frac{d}{2}\right) \approx \frac{cH_a}{4\pi}\frac{x}{\sqrt{w^2-x^2}}. \tag{4}$$

On the other hand, at $t^2 \gtrsim 1$, i.e., at $w - x \lesssim d$, formula (2) gives

$$\frac{w-x}{w} \approx \frac{m}{2}|t|\sqrt{t^2-1} - \frac{m}{2}\ln[|t| + \sqrt{t^2-1}]. \tag{5}$$

Thus, formulas (1), (3), and (5) provide an explicit description in the parametric form of the surface currents in the edge region of the strip. In particular, near a corner of the sample (at $l \equiv w - x \ll d$, or at $l \equiv d/2 - |y| \ll d/2$), we obtain that the surface current diverges like $l^{-1/3}$:

$$J \approx \frac{cH_a}{4\pi\sqrt{m}}\left(\frac{2d}{3\pi l}\right)^{1/3}. \tag{6}$$

Of course, this divergence should be cut off at $l \lesssim \lambda$, and the current density j throughout the corner region ($w - \lambda \le x \le w$, $d/2 - \lambda \le |y| \le d/2$) is approximately constant and is of the order of

$$j(x, y) \sim \frac{J(x = w-\lambda)}{\lambda} \approx \frac{cH_a}{4\pi\lambda\sqrt{m}}\left(\frac{2d}{3\pi\lambda}\right)^{1/3}. \tag{7}$$

3. THE PENETRATION FIELD

3.1. Bean–Livingston Barrier

Using the results in Sec. 2, we now estimate the penetration field H_p^{BL} that is due to the Bean–Livingston barrier originating on the scale λ from the surface. Since the Meissner currents are maximum at the corners of the sample, it is favorable for a vortex to penetrate into the strip through these points. We consider a small circular vortex arc of radius $r < \lambda$ with its focal point placed at a corner of the strip (in estimating H_p^{BL}, we assume that $\xi \ll \lambda$ for simplicity). The effect of the surfaces of the superconductor on the vortex segment can be taken into account by constructing the images of the arc. This trick ensures that the currents generated by the vortex are tangential to the surface [1]. The energy of the vortex arc calculated within this approach also largely takes the stray fields outside the sample into account [39]. Therefore, the energy $E_{\rm arc}$ of the penetrating vortex arc can be estimated as a quarter of the energy of the appropriate circular vortex ring placed in the bulk of the superconductor [40, 41],

$$E_{\rm arc}(r) \approx \frac{\pi}{2}r\varepsilon_0\left[\ln\left(\frac{r}{\xi}\right) + c_0\right], \tag{8}$$

where $\varepsilon_0 = \Phi_0^2/(4\pi\lambda)^2$, the factor $\ln(r/\xi)$ takes into account that the magnetic fields and currents begin to decay sharply at the distance r from the ring rather than at the distance λ, and the constant c_0 determines the energy of the ring of the radius $r = \xi$. This constant c_0 is given by the formula [40, 41],

$$c_0 \approx \frac{\pi}{\kappa}\int_0^\kappa dq\frac{[J_1(q/\kappa)]^2}{\sqrt{1+q^2}} = \pi\int_0^1 du\frac{u[J_1(u)]^2}{\sqrt{\kappa^{-2}+u^2}}, \tag{9}$$

where $J_1(x)$ is the Bessel function of the first kind. At $\kappa \gg 1$, the constant c_0 is practically independent of κ, and we have $c_0 \approx 0.22$.

At a given current density j, there is a critical radius r_c at which the Lorentz force $(j\Phi_0/c)\pi r_c/2$ generated by the current and acting on the vortex is balanced by the squeezing force $-\partial E_{\rm arc}/\partial r$. In other words, this $r_c(j)$ is found from the equation

$$\frac{1}{2c}j\Phi_0\pi r_c = \frac{\pi}{2}\varepsilon_0\left[\ln\left(\frac{r_c}{\xi}\right) + 1 + c_0\right].$$

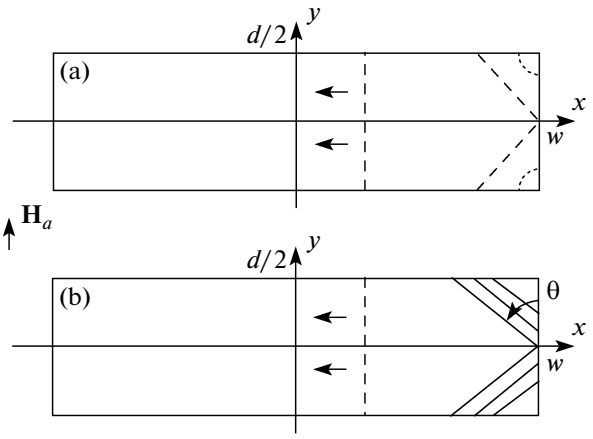

Fig. 2. Two scenarios of vortex penetration into the strip. (a) $p > p_c$, the Bean–Livingston barrier prevails over the geometric one. (b) $p < p_c$, the penetration of vortices is mainly determined by the geometric barrier. The parameter p is defined by Eq. (19), $p_c \approx 0.52$. The dashed lines schematically show vortices propagating in the strip. The solid lines inside the strip designate the immobile vortices that are in equilibrium. These vortices form flux-line domes near the edges of the strip.

If $r > r_c$, the vortex arc expands, and the quantity

$$U_c(j) = E_{\rm arc}(r_c) - j\Phi_0\pi r_c^2/4c$$

specifies the height of the Bean–Livingston barrier near the corner. When the current density j increases, the radius r_c and $U_c(j)$ decrease, and the barrier U_c disappears at $r_c \approx \xi\exp(1-c_0) \approx 2.2\xi$. The appropriate j is of the order of the depairing current density,

$$j = 2e^{-(1-c_0)}\frac{c\varepsilon_0}{\Phi_0\xi} \approx \frac{0.92cH_{c1}\kappa}{4\pi\lambda\ln\kappa}, \qquad (10)$$

whereas $4\pi j\lambda/c$, the local surface field near the corner, reaches the value of the thermodynamic critical field in agreement with the results in [32, 39, 42, 43]. Equating this j to the current density defined by Eq. (7), we find the penetration field $H_a = H_p^{BL}$ at which the Bean–Livingston barrier disappears for a vortex penetrating through a sample corner,

$$H_p^{BL} \approx \frac{0.92H_{c1}\kappa}{\ln\kappa}\left(\frac{18d\lambda^2}{\pi w^3}\right)^{1/6}. \qquad (11)$$

We note that due to a small value of the ratio λ/d, this penetration field is noticeably smaller not only than the common $H_p^{BL} \approx H_{c1}\kappa/\ln\kappa$ but also than the field of a vortex penetration through the equatorial point $t = 0$ of the lateral surface of the strip,

$$\frac{H_{c1}\kappa}{\ln\kappa}\left(\frac{2d}{\pi w}\right)^{1/2}.$$

This estimate is obtained by equating the depairing current density to $J(0)/\lambda$, where $J(0)$ is taken from Eq. (3).

3.2. Geometric Barrier Within a Simplified Approach

We now calculate the penetration field caused exclusively by the geometric barrier in a thin strip, neglecting the attraction of vortices to the surfaces of the strip. In this case, a penetrating vortex can jump to the center of the sample only when its two rectilinear segments meet at the equatorial point ($x = w$, $y = 0$), as shown in Fig. 2. Let us consider a vortex that ends at the point x_0 of the lower plane of the strip and at the point y_0 of its lateral surface. The balance between the line tension of the vortex and the forces generated by the surface currents leads to the following equations for x_0, y_0, θ and H_a:

$$\begin{aligned}\frac{1}{c}\Phi_0 J\left(x_0, -\frac{d}{2}\right) &= e_0\sin\theta,\\ \frac{1}{c}\Phi_0 J(w, y_0) &= e_0\cos\theta,\end{aligned} \qquad (12)$$

where the sheet currents $J(x, y)$ are determined by the formulas in Sec. 2, $e_0 = \varepsilon_0\ln\kappa$, and $\theta < \pi/2$ is the tilt angle of the vortex relative to the lateral surface of the strip (see Fig. 2). An inspection of Fig. 2 also gives a geometric relation between x_0, y_0, and θ,

$$w - x_0 = \left(\frac{d}{2} + y_0\right)\tan\theta. \qquad (13)$$

Because $y_0 = 0$ at the penetration field, Eqs. (12) and (13) completely determine the three quantities θ, $H_a = H_p$, and x_0.

We rewrite these equations using formulas of Section 2. Then Eqs. (12) become

$$\cos\theta = \frac{\sqrt{1-mt^2}}{\sqrt{1-t^2}}h, \qquad (14)$$

$$\sin\theta = \frac{\sqrt{1-mt_1^2}}{\sqrt{t_1^2-1}}h, \qquad (15)$$

where $m \approx 2d/\pi w$, $h \equiv \tilde{H}_a/\sqrt{m}$, $\tilde{H}_a \equiv H_a/H_{c1}$ is the dimensionless applied magnetic field, and the parameters $t < 1$ and $t_1 > 1$ respectively correspond to the points y_0 and x_0. Equation (13) with the use of formulas (1) and (5) gives

$$\begin{aligned}&[t_1\sqrt{t_1^2-1} - \ln(t_1 + \sqrt{t_1^2-1})]\\ &= \left(\frac{\pi}{2} - \arcsin(t) - t\sqrt{1-t^2}\right)\tan\theta.\end{aligned} \qquad (16)$$

Besides, we can set $\sqrt{1-mt^2} \approx \sqrt{1-mt_1^2} \approx 1$ in Eqs. (14) and (15) since $m \ll 1$, $t < 1$, and $t_1 \sim 1$ here. Then Eqs. (14)–(16) become independent of m, and the aspect ratio d/w specifies only the normalization factor in the definition of h.

At the penetration field, we have $t = 0$, and Eqs. (14) and (15) give $h \approx \cos\theta$ and $t_1^2 \approx 1 + \cot^2\theta$. Eventually, Eq. (16) reduces to an equation for the angle θ,

$$\frac{\pi}{2}\tan\theta = \cot\theta\sqrt{1+\cot^2\theta} - \ln(\cot\theta + \sqrt{1+\cot^2\theta}), \quad (17)$$

which gives $\tan\theta \approx 0.74$ ($\theta \approx 36.5°$). Hence, from $h \approx \cos\theta$, we obtain the penetration field caused by the geometric barrier

$$H_p^{GB} \approx H_{c1}\sqrt{m}\cos\theta, \quad (18)$$

where $\cos\theta \approx 0.80$. The obtained H_p^{GB} has the same order of magnitude as the penetration field found in [2, 3]. However, we emphasize that estimate (18) is derived for a single vortex reaching the equator. Such a situation does not actually occur, as is described in the next section. We also note that at the penetration field given by Eq. (18), the surface current $J(0)$ at the equatorial point $(x = w, y = 0)$ is equal to $cH_{c1}\cos\theta/4\pi$.

3.3. Two Scenarios of Vortex Penetration

The comparison of formulas (11) and (18) shows that the ratio of H_p^{BL} and H_p^{GB} is equal to p/p_c where the parameter p is defined as

$$p \equiv \frac{\kappa}{\ln\kappa}\left(\frac{\lambda}{d}\right)^{1/3}, \quad (19)$$

and

$$p_c = \left(\frac{2}{3\pi}\right)^{1/3}\frac{2\cos\theta}{\exp(1-c_0)} \approx 0.52.$$

If the parameter p is larger than its critical value p_c, we have $H_p^{BL} > H_p^{GB}$, and the penetration field H_p coincides with H_p^{BL}:

$$H_p = H_p^{BL} \approx H_{c1}\sqrt{m}\frac{0.8p}{p_c}, \quad p \geq p_c. \quad (20)$$

In this case, small vortex segments appearing at the corners of the strip at $H_a = H_p^{BL}$ immediately expand, merge at the equatorial point $(x = w, y = 0)$, and the created vortex jumps to the center of the sample (see Fig. 2). This type of penetration occurs because at $p > p_c$ and $H_a = H_p^{BL}$, when the current density in the corner region is close to the depairing current density, the surface current $J(0)$ at the equatorial point is larger than $cH_{c1}\cos\theta/4\pi$, and the vortex end cannot be in equilibrium at this point. At $H_a > H_p$, the vortex dome appearing in the center of the strip is quite similar to the dome described previously [2], even though the penetration field is now determined by the Bean–Livingston barrier. This is because the dome is determined by the Meissner currents flowing far away from the edges of the strip.

If the parameter p is less than the critical value p_c, we have $H_p^{BL} < H_p^{GB}$, and the vortex penetration is a two-stage process. The current density in the vicinity of the corners reaches the depairing value at $H_a = H_p^{BL}$. At this field, a penetrating vortex line enters the sample through the corner, but it cannot reach the point $(x = w, y = 0)$ because $J(0)$ is less than $cH_{c1}\cos\theta/4\pi$, and hence this line "hangs" between the corner and the equatorial point $(x = w, y = 0)$. With increasing H_a, two domes filled by these inclined lines expand in the lateral surface of the strip. The penetration field H_p is determined by the condition that the boundaries of these domes meet at a equatorial point, and at this field, a dome in the center of the strip begins to form. But the value of H_p, strictly speaking, is different from that given by Eq. (18) since the vortex domes near the edges of the strip modify the current distribution, and therefore H_p has to be calculated self-consistently (see Sec. 4). Interestingly, if $(\lambda/d)^{1/3} \geq 0.2$, we obtain that $p > p_c$ for any $\kappa > 1$. Therefore, for the case $p < p_c$ to be possible at a given κ, the sample should be thick enough compared to λ.

4. SELF-CONSISTENT CALCULATION OF THE PENETRATION FIELD H_p AT $p < p_c$

We consider the case $p < p_c$, when the domes of the tilted vortex lines appear on the lateral surfaces of the strip in an increasing applied magnetic field. In this situation, the surface currents in the sample are composed of the part that screens the applied magnetic field H_a and the part generated by the vortices. The first part was calculated in Sec. 2, while the second part can be found using formulas in the Appendix. Let the ends of a vortex be at the point $(x = w, y = y_0)$ of the lateral surface of the strip and the point $(x = x_0, y = -d/2)$ of its lower plane. (In reality, we consider a vortex "layer" extending in the z direction and consisting of such inclined vortices.) According to Eqs. (12), for this vortex to be in equilibrium, the surface currents must be equal to $cH_{c1}\cos\theta/4\pi$ at the point $(x = w, y = y_0)$ and to $cH_{c1}\sin\theta/4\pi$ at the point $(x = x_0, y = -d/2)$. Then Eqs. (12) take the form

$$\cos\theta = \frac{\sqrt{1-mt^2}}{\sqrt{1-t^2}}[h + F(t)], \quad (21)$$

$$\sin\theta = \frac{\sqrt{1-mt_1^2}}{\sqrt{t_1^2-1}}[h + F(t_1)], \quad (22)$$

where $h = H_a/\sqrt{m}\,H_{c1}$, and the first terms in the right-hand sides of these equations describe the Meissner currents that were solely taken into account in deriving

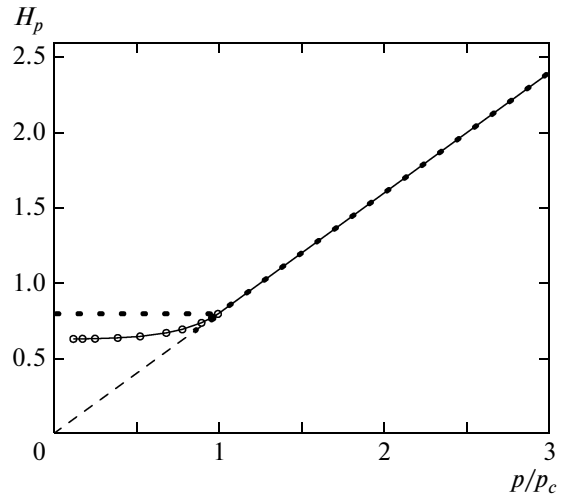

Fig. 3. The penetration field H_p (the solid line) as a function of the parameter p defined by Eq. (19). The line with circles is the function $f(p/p_c)$ in Eq. (26), and the line with dots at $p/p_c > 1$ is given by formula (20). The dashed line is the extrapolation of dependence (20) to the region $p < p_c$. The dotted line shown $H_p(p)$ according to Eq. (18) with $\cos\theta = 0.80$. The field H_p is measured in units of $H_{c1}\sqrt{m}$.

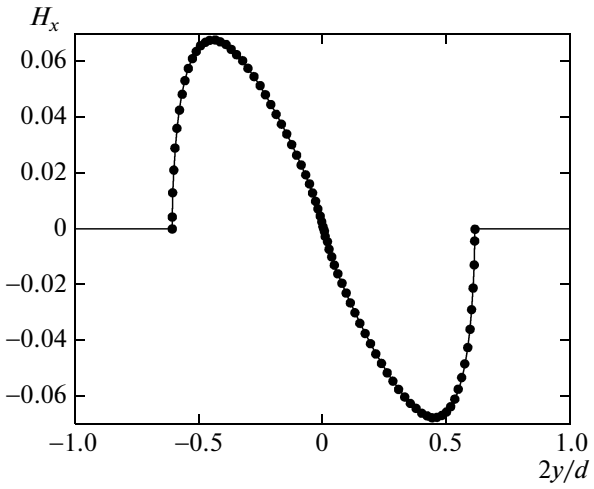

Fig. 4. The profile $H_x(y)$ on the lateral surface of the strip at $H_a = H_p$ for $p/p_c = 0.895$. This p corresponds to $H_p = 0.737H_{c1}\sqrt{m}$, $t_u = 0.5$, and $2y(t_u)/d \approx 0.609$. The field H_x is measured in units of H_{c1}.

H_p^{GB} in Sec. 3.2. The second terms describe the currents generated by the inclined vortices,

$$F(t) \equiv \frac{2}{\pi}\int_{t_d}^{t_u} dt'\,\tilde{H}_x(t')\sqrt{1-(t')^2} \times \frac{(t_1'-t')(t't_1'+t^2)}{[t^2-(t_1')^2][t^2-(t')^2]}, \quad (23)$$

where $\tilde{H}_x = H_x/H_{c1}$ and H_x is the x-component of the magnetic field at the lateral surface $x = w$. This component is due to the tilt of the vortices and is perpendicular to this surface. In Eqs. (21)–(23), the coordinates x_0 and y_0 are expressed in terms of the parameters t and t_1 used in Sec. 3.2. Due to geometric condition (16), the parameters t_1, t, and θ are interconnected (the same is true for t', t_1', and θ' in the integrand in Eq. (23)). The integration in Eq. (23) is carried out over the vortex dome, $t_d \le t \le t_u$, located in the lower part of the lateral surface of the strip. The boundaries of this dome, t_d and t_u, are found from the conditions that the current density J/λ at the distance λ from the corner be equal to the current density defined by Eq. (10),

$$h + F(1) = \frac{H_p^{BL}}{H_{c1}\sqrt{m}} \approx \frac{0.8p}{p_c}, \quad (24)$$

and that

$$\tilde{H}_x = 0 \quad (25)$$

at $t = t_d$ and $t = t_u$.

When $H_a = H_p^{BL}$ (the dashed line in Fig. 3), we have $F(1) = 0$ from Eq. (24). This means that $t_d = t_u$, i.e., the dome only begins to form at this magnetic field. We can then omit the function $F(t)$ in Eqs. (21) and (22). These equations together with formula (16) allow finding $t = t_d = t_u$ and also t_1 and θ in the manner similar to that in Sec. 3.2. In other words, we can find the point on the lateral surface of the strip where the dome begins to form. With increasing H_a, the difference $t_u - t_d$ increases, and the parameter t_d reaches zero at $H_a = H_p$. Thus, H_p can be found from Eqs. (16), (21)–(25) if we set $t_d = 0$ in Eq. (23). Eventually, we find

$$H_p = H_{c1}\sqrt{m}f\left(\frac{p}{p_c}\right), \quad p \le p_c, \quad (26)$$

where the function $f(u)$ calculated numerically is shown in Fig. 3. It can be seen that in the self-consistent calculation, $H_p/H_{c1}\sqrt{m}$ decreases compared to the value 0.8 that follows from Eq. (18). As $p \longrightarrow 0$, we now have $H_p/H_{c1}\sqrt{m} \approx 0.63$. As an example, in Figs. 4 and 5 we show the dependences $\tilde{H}_x(y)$ and $\theta(y)$ obtained by solving Eqs. (16), (21)–(25) at $t_d = 0$ with $p/p_c = 0.895$. We note that the field $H_x(y)$ in the vortex dome formed on the lateral surface has opposite signs above and below the equator and vanishes at $y = 0$.

The tilted vortices starting on the lateral surfaces of the sample also form the domes $H_y(x)$ on the upper (lower) surfaces of the strip near its corners. The shape of these domes can be found from the obtained profiles

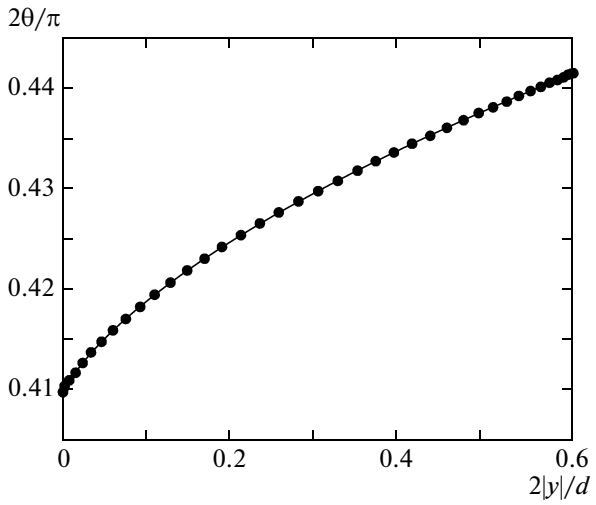

Fig. 5. The profile $\theta(y)$ on the lateral surface of the strip at $H_a = H_p$ for $p/p_c = 0.895$.

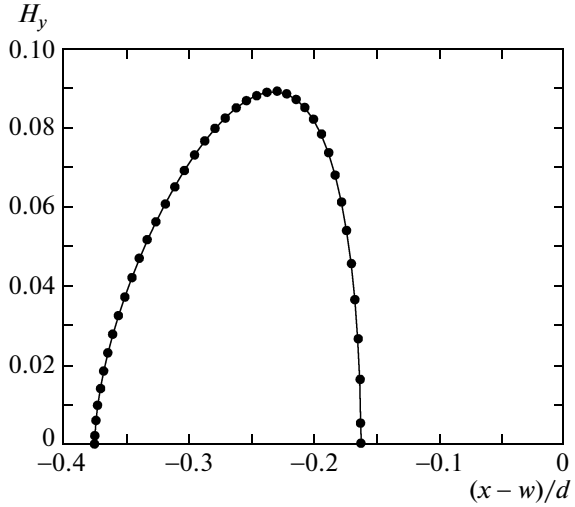

Fig. 6. The profile $H_y(x)$ on the upper surface of the strip at $H_a = H_p$ for $p/p_c = 0.895$. The field H_y is measured in units of H_{c1}.

$H_x(y)$ and $\theta(y)$ using the conservation of the flux and relation (16), Fig. 6. We note that the derived edge dome in Fig. 6 is a unique feature of the combined effect of surface and geometric barriers and is very different from the edge field distribution obtained in [2] and [3], which increases monotonically and diverges at the sample corners.

We assumed above that the tilted vortices penetrating the lateral surface of the strip are straight, see Eq. (16). This assumption is indeed justified under the condition $B \ll H_{c1}$ implied throughout the paper. In this case, we have [44, 45] $\mathbf{H} = H\mathbf{n} \approx H_{c1}\mathbf{n}$ for the thermodynamic magnetic field $\mathbf{H} = 4\pi\partial F/\partial\mathbf{B}$, where $F(B)$ is the free-energy density, $\mathbf{n} \equiv \mathbf{B}/B = (\cos\theta, \sin\theta, 0)$ is the unit vector along $\mathbf{B}$, and the angle $\theta(x, y)$ defines the local direction of a vortex at the point (x, y). The shape of the vortex lines inside a superconductor in the absence of pinning is determined by the equations $\mathrm{div}\,\mathbf{B} = 0$ and $\mathrm{curl}\,\mathbf{H} = 0$ [46]. The last of these equations gives $(\mathbf{n}\cdot\nabla)\theta = 0$, which means that the angle θ is indeed a constant along any tilted vortex crossing the lateral surface of the strip.

5. DISCUSSION

We compare the magnetic moment of the strip (calculated per unit length along the z axis) in the cases $p > p_c$ and $p < p_c$. In the first case ($p > p_c$), when the penetration field H_p is determined by the Bean–Livingston barrier, the magnetic moment of the strip in the Meissner state, i.e., at $H_a < H_p$, is equal to [38]

$$M_y = -\frac{w^2(1-m)H_a}{4[E(k') - mK(k')]^2} \approx -\frac{H_a w^2}{4}, \qquad (27)$$

where $m \approx 2d/\pi w$, $k' \equiv \sqrt{1-m}$, and $K(k')$ and $E(k')$ are the complete elliptic integrals of the first and second kinds, respectively. In the second case ($p < p_c$), when the penetration field is determined by the geometric barrier, the magnetic moment is still given by formula (27) at $H_a \le H_p^{BL}$, where H_p^{BL} is described by Eq. (11) or Eq. (20). But at $H_p^{BL} < H_a < H_p$, an additional contribution δM_y to the magnetic moment appears. This contribution is due to the currents generated by the domes of the tilted vortices. The accurate analysis of δM_y requires substantial numerical calculations, and we here give only a simple estimate of this δM_y,

$$\frac{|\delta M_y|}{M_y} \sim \sqrt{m}\left(1 - 0.8\frac{p}{p_c h}\right) \ll 1, \qquad (28)$$

where $h = H_a/\sqrt{m}\,H_{c1}$. Hence, a small break in the H_a-dependence of the magnetic moment should occur at $H_a = H_p^{BL}$ in the second case, $p < p_c$. Because the parameter p increases with increasing the temperature T due to the increase in $\lambda(T)$, the second type of the vortex penetration transforms into the first type with increasing T. In this situation, if the temperature dependence of the magnetic moment M_y is measured at a constant H_a, a break in this dependence $M(T)$ should also occur.

When H_a exceeds H_p, the vortex dome in the center of the strip begins to form. The boundary b of this dome is found from the condition that the current density J/λ at the distance λ from the corner is equal to the current density defined by Eq. (10), whereas the shape of the vortex dome at $|x| \le b$ is determined by the equation $J(x, d/2) = J(x, -d/2) = 0$. The difference between the cases $p > p_c$ and $p < p_c$ is only in that the currents generated by the domes of the tilted vortices must be taken into account in the second case. But if

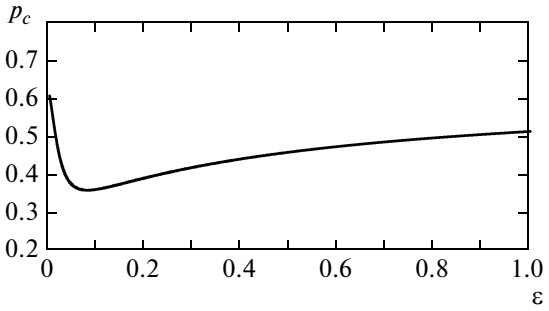

Fig. 7. The dependence of the critical value p_c on the anisotropy parameter ε under the condition that H_p^{BL} is independent of ε. Here, $m = 1/36$ i.e., $w/d \approx 22.9$.

$H_p < H_a \ll H_{c1}$, then the domes near the edges of the strip and at its center are far from each other, and we can neglect their mutual influence in the first approximation. In this situation, the domes near the edges of the sample do not change with increasing H_a, and the distinction between the central domes for $p > p_c$ and $p < p_c$ is small. Using formula (34), we can show that these central domes are approximately described by the appropriate formula in [2]. When $H_a \sim H_{c1}$, the central dome and the domes near the edges of the strip are close to each other, and any of them should be calculated self-consistently, taking the effect of the other domes into account. This situation will be considered elsewhere.

So far, we have considered the vortex penetration into an isotropic superconducting strip. We now briefly discuss the case of an anisotropic superconductor, where the anisotropy parameter $\varepsilon \equiv \lambda_{ab}/\lambda_c$ is less than unity, $\varepsilon < 1$. Here, λ_{ab}, and λ_c are the respective London penetration depths in the plane of the strip and in the direction perpendicular to this plane. Because the field H_p^{BL} is determined by the depairing current density (see Sec. 3.1), we can expect that this field is practically independent of ε. With formulas of [47], it can be shown that the anisotropy ε leads to the respective additional factors $1/\epsilon_\theta$ and $\varepsilon^2/\epsilon_\theta$ in the left-hand sides of Eqs. (14) and (15), where $\epsilon_\theta \equiv \sqrt{\cos^2\theta + \varepsilon^2 \sin^2\theta}$. As a result, the field H_p^{GB} found in Sec. 3.2 depends on ε. But this dependence proves to be relatively weak, and hence the critical value p_c introduced in Sec. 3.3 as the ratio H_p^{BL}/H_p^{GB} also depends on ε weakly (Fig. 7). Therefore, $p_c(\varepsilon)$ is of the same order of magnitude as in the isotropic case $\varepsilon = 1$. This result means that we have $p > p_c$ for anisotropic superconductors with $\kappa \gg 1$ at reasonable ratios λ_{ab}/d.

6. SUMMARY

We analyzed the process of vortex penetration into a thin superconducting strip of a rectangular cross section, with the width and the thickness of the strip being much larger than the London penetration depth. It is shown that in the absence of flux-line pinning, the process of penetration is governed by the parameter p, Eq. (19), characterizing an interplay between the Bean–Livingston and geometric barriers. If this parameter is larger than the critical value $p_c \sim 0.52$, the magnitude H_p of the external magnetic field at which the vortex penetration into the central region of the sample starts is determined by the Bean–Livingston barrier in the corners of the strip, $H_p = H_p^{BL}$, and is given by Eq. (11) or, equivalently, by Eq. (20). At an external magnetic field $H_a \geq H_p$, the vortex dome in the center of the strip forms, and its shape is close to that described previously [2]. In the opposite situation where $p < p_c$, we obtain $H_p > H_p^{BL}$ (see Fig. 3), and the vortex penetration is a two-stage process. In the interval $H_p^{BL} < H_a < H_p$, the tilted vortices penetrate only into the edge regions of the strip, and vortex domes of unusual shape appear there (see Fig. 4 and 6). At $H_a \geq H_p$, the edge domes practically do not change, whereas the vortex dome in the center of the strip develops. The shape of this central dome is again close to that described previously [2]. Hence, two types of vortex domes exist in the sample in this case.

In principle, the predicted new edge domes should be observable experimentally by decorations, magneto–optics, and scanning SQUID microscopy. These domes change currents circulating in the sample. Hence, if the edge vortex domes appear or disappear in a superconductor under changes of the external magnetic field H_a or the temperature T, the magnetic moment M of the sample should exhibit a small break in the appropriate H_a- or T-dependences of M.

ACKNOWLEDGMENTS

We thank I. M. Babich for the helpful discussions. This work was supported by the German–Israeli Foundation for Scientific Research and Development (GIF).

APPENDIX

Currents Generated by "Layers" of Tilted Vortices in a Strip

We consider two thin "layers" of tilted vortices in the lower part of the strip (Fig. 8a). These two layers are located symmetrically with respect to the axis $x = 0$, and extend to infinity in the z direction. Let the ends of the right layer be at the points (w, y_0) and $(x_0, -d/2)$ described by the respective parameters t'

and t_1'. The width of the layer is determined by the small interval dt' or by the appropriate dy_0, and the layer carries the magnetic flux $d\Phi = H_x(y_0)dy_0$. The surface currents generated by the two layers can be found using the results of Sec. 2 and a conformal map that transforms the upper half-plane of the complex plane onto the interior of the rectangle shown in Fig. 8b. The lower and upper sides of this rectangle correspond to the parts of the magnetic field lines $A = 0$ and $A = -d\Phi$ that lie outside the strip and that are shown in Fig. 8a, while the lateral sides of the rectangle correspond to the infinitesimal intervals dy_0 and dx_0 carrying the flux $d\Phi$. Eventually, we find that the surface current generated by the layers at a point t is given by

$$\frac{4\pi}{c}J(t) = G(t')\left(\frac{1-mt^2}{1-t^2}\right)^{1/2}\frac{t_1'-t'}{[t_1'-t][t-t']} \qquad (29)$$

if $-1 \le t \le 1$, and by

$$\frac{4\pi}{c}J(t) = \mathrm{sgn}(t)G(t')\left(\frac{1-mt^2}{t^2-1}\right)^{1/2}\frac{t_1'-t'}{[t_1'-t][t-t']} \qquad (30)$$

if $1 \le |t| \le 1/\sqrt{m}$. Here, $\mathrm{sgn}(t) = 1$ for $t > 0$ and $\mathrm{sgn}(t) = -1$ for $t < 0$, the factor $G(t')$ is

$$G(t') = \frac{H_x(t')dt'}{\pi}\left(\frac{1-(t')^2}{1-m(t')^2}\right)^{1/2}, \qquad (31)$$

and $H_x(t') = H_x(y_0)$.

If two similar layers are in the upper part of the strip, i.e., if the right layer has the coordinates $-t'$ and $-t_1'$ and carries the flux $H_x(-t')dy_0 = -H_x(t')dy_0 = -d\Phi$, then we find

$$\frac{4\pi}{c}J(t) = -G(t')\left(\frac{1-mt^2}{1-t^2}\right)^{1/2}\frac{t_1'-t'}{[t_1'+t][t+t']} \qquad (32)$$

for $-1 \le t \le 1$ and

$$\frac{4\pi}{c}J(t) = -\mathrm{sgn}(t)G(t')\left(\frac{1-mt^2}{t^2-1}\right)^{1/2}\frac{t_1'-t'}{[t_1'+t][t+t']} \qquad (33)$$

for $1 \le |t| \le 1/\sqrt{m}$. Formula (23) is the sum of the expressions (29) and (32) and also (30) and (33) for $t > 0$.

In a similar manner, we can obtain the surface currents generated by two vertical layers of vortices that are located symmetrically with respect to the axis $x = 0$. Let the ends of the right layer be at the points $(x_0, -d/2)$ and $(x_0, d/2)$ described by the respective parameters t_1' and $-t_1'$. The width of the layer is determined by the small interval dt_1' or by the appropriate dx_0, and the layer carries the magnetic flux $d\Phi = H_y(x_0)dx_0$. Eventually, we find the following surface currents generated by the layers at a point t_1 on the upper or lower surfaces of the strip, $1 \le |t_1| \le 1/\sqrt{m}$,

$$\frac{4\pi}{c}J(u) = -\frac{2}{\pi}H_y(u')du'\left(\frac{1-(u')^2}{1-u^2}\right)^{1/2} \times \frac{u}{u^2-(u')^2}, \qquad (34)$$

where $u \equiv \sqrt{1-mt_1^2}/\sqrt{1-m}$, $u' = u(t_1')$, and $H_y(u') = H_y(t_1') = H_y(x_0)$. When x_0 is not close to the edge of the strip ($w - x_0 \gg d$), we have $u \approx x_0/w$ (see Sec. 2).

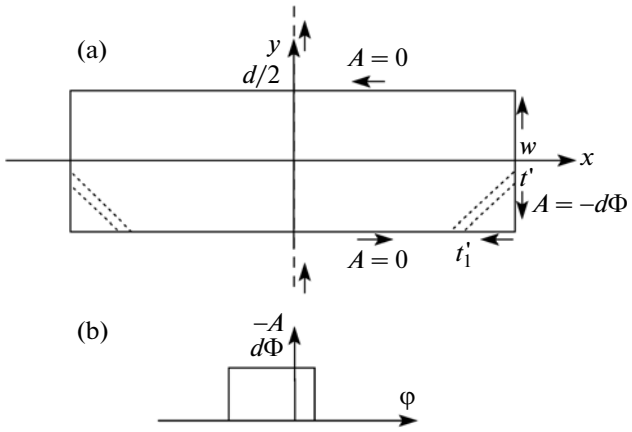

Fig. 8. (a) Two thin symmetric layers of tilted vortices penetrating the lower part of the strip are shown schematically as the dashed lines. The ends of the right layer carrying the flux $d\Phi$ are marked by t' and t_1'. Arrows indicate directions of the magnetic field lines $A = 0$ and $A = -d\Phi$ that leave and enter the right layer and that adjoin the surface of the strip (the line $A = 0$ also passes through the infinite point). (b) The rectangle in the complex plane $\varphi - iA$ (see the text).

REFERENCES

1. C. P. Bean and J. D. Livingston, Phys. Rev. Lett. **12**, 14 (1964).
2. E. Zeldov, A. I. Larkin, V. B. Geshkenbein, M. Konczykowski, D. Majer, B. Khaykovich, V. M. Vinokur, and H. Shtrikman, Phys. Rev. Lett. **73**, 1428 (1994).
3. E. Zeldov, A. I. Larkin, M. Konczykowski, B. Khaykovich, D. Majer, V. B. Geshkenbein, and V. M. Vinokur, Physica C (Amsterdam) **235–240**, 2761 (1994).
4. J. R. Clem, in *Proceedings of the 13th Conference on Low Temperature Physics (LT13), Boulder, Colorado, United States, August 21–25, 1972*, Ed. by K. D. Thimmerhaus, W. J. O'Sullivan, and E. F. Hammel (Plenum, New York, 1974), Vol. 3, p. 102.
5. M. Benkraouda and J. R. Clem, Phys. Rev. B: Condens. Matter **53**, 5716 (1996).

6. E. H. Brandt, Phys. Rev. B: Condens. Matter **59**, 3369 (1999).
7. E. H. Brandt, Phys. Rev. B: Condens. Matter **60**, 11939 (1999).
8. L. Burlachkov, Phys. Rev. B: Condens. Matter **47**, 8056 (1993).
9. L. Burlachkov, V. B. Geshkenbein, A. E. Koshelev, A. I. Larkin, and V. M. Vinokur, Phys. Rev. B: Condens. Matter **50**, 16670 (1994).
10. M. Yu. Kupriyanov and K. K. Likharev, Sov. Phys. Solid State **16** (10), 1835 (1975).
11. L. Burlachkov, A. E. Koshelev, and V. M. Vinokur, Phys. Rev. B: Condens. Matter **54**, 6750 (1996).
12. M. Benkraouda and J. R. Clem, Phys. Rev. B: Condens. Matter **58**, 15103 (1998).
13. A. A. Elistratov, D. Yu. Vodolazov, I. L. Maksimov, and J. R. Clem, Phys. Rev. B: Condens. Matter **66**, 220506(R) (2002).
14. M. Konczykowski, L. I. Burlachkov, Y. Yeshurun, and F. Holtzberg, Phys. Rev. B: Condens. Matter **43**, 13707 (1991).
15. N. Chikumoto, M. Konczykowski, N. Motohira, and A. P. Malozemoff, Phys. Rev. Lett. **69**, 1260 (1992).
16. M. Indenbom, H. Kronmuller, T. W. Li, P. H. Kes, and A. A. Menovskii, Physica C (Amsterdam) **222**, 203 (1994).
17. M. Marchevsky, L. A. Gurevich, P. H. Kes, and J. Aarts, Phys. Rev. Lett. **75**, 2400 (1995).
18. D. Majer, E. Zeldov, and M. Konczykowski, Phys. Rev. Lett. **75**, 1166 (1995).
19. Y. C. Kim, J. R. Thompson, D. K. Christen, Y. R. Sun, M. Paranthaman, and E. D. Specht, Phys. Rev. B: Condens. Matter **52**, 4438 (1995).
20. R. B. Flippen, T. R. Askew, J. A. Fendrich, and C. J. van der Beek, Phys. Rev. B: Condens. Matter 52, R9882 (1995).
21. N. Morozov, E. Zeldov, D. Majer, and B. Khaykovich, Phys. Rev. Lett. **76**, 138 (1996).
22. N. Morozov, E. Zeldov, M. Konczykowski, and R. A. Doyle, Physica C (Amsterdam) **291**, 113 (1997).
23. Y. Paltiel, D. T. Fuchs, E. Zeldov Y. N. Myasoedov, H. Shtrikman, M. L. Rappaport, and E. Andrei, Phys. Rev. B: Condens. Matter **58**, R14763 (1998).
24. D. T. Fuchs, E. Zeldov, M. Rappaport, T. Tamegai, S. Ooi, and H. Shtrikman, Nature (London) **391**, 373 (1998).
25. D. T. Fuchs, R. A. Doyle, E. Zeldov, S. F. W. R. Rycroft, T. Tamegai, S. Ooi, M. L. Rappaport, and Y. Myasoedov, Phys. Rev. Lett. **81**, 3944 (1998).
26. P. K. Mishra, G. Ravikumar, T. V. C. Rao, V. C. Sahni, S. S. Banerjee, S. Ramakrishnan, A. K. Grover, and M. J. Higgins, Physica C (Amsterdam) **340**, 65 (2000).
27. Z. L. Xiao, E. Y. Andrei, Y. Paltiel, E. Zeldov, P. Shuk, and M. Greenblatt, Phys. Rev. B: Condens. Matter **65**, 094511 (2002).
28. A. A. F. Olsen, H. Hauglin, T. H. Johansen, P. E. Goa, and D. Shantsev, Physica C (Amsterdam) **408–410**, 537 (2004).
29. L. Lyard, T. Klein, J. Markus, R. Brusetti, C. Marcenat, M. Konczykowski, V. Mosser, K. H. Kim, B. W. Kang, H. S. Lee, and S. I. Lee, Phys. Rev. B: Condens. Matter **70**, 180504(R) (2004).
30. H. Beidenkopf, Y. Myasoedov, E. Zeldov, E. H. Brandt, G. P. Mikitik, T. Tamegai, T. Sasagawa, and C. J. van der Beek, Phys. Rev. B: Condens. Matter **80**, 224526 (2009).
31. Y. Segev, I. Gutman, S. Goldberg, Y. Myasoedov, E. Zeldov, E. H. Brandt, G. P. Mikitik, T. Katagiri, and T. Sasagawa, Phys. Rev. B: Condens. Matter **83**, 104520 (2011).
32. P. G. de Gennes, *Superconductivity of Metals and Alloys* (W. A. Benjamin, New York, 1966).
33. V. G. Kogan, Phys. Rev. B: Condens. Matter **49**, 15874 (1994).
34. I. L. Maksimov and A. A. Elistratov, JETP Lett. **61** (3), 208 (1995).
35. A. I. Larkin and Yu. N. Ovchinnikov, Sov. Phys. JETP **34**, 651 (1972).
36. L. D. Landau and E. M. Lifshitz, *Course of Theoretical Physics*, Volume 8: *Electrodynamics of Continuous Media* (Pergamon, London, 1959).
37. M. A. Lavrentiev and B. V. Shabat, *Methods of the Theory of Functions of a Complex Variable* (Nauka, Moscow, 1987) [in Russian].
38. E. H. Brandt and G. P. Mikitik, Phys. Rev. Lett. **85**, 4164 (2000).
39. A. V. Samokhvalov, JETP **81** (3), 601 (1995).
40. V. A. Kozlov and A. V. Samokhvalov, JETP Lett. **53** (3), 158 (1991).
41. V. A. Kozlov and A. V. Samokhvalov, Physica C (Amsterdam) **213**, 103 (1993).
42. V. P. Galaiko, Sov. Phys. JETP **23** (5), 878 (1966).
43. Y. A. Genenko, Phys. Rev. B: Condens. Matter **49**, 6950 (1994).
44. M. Tinkham, *Introduction to Superconductivity* (McGraw-Hill, New York, 1996).
45. E. H. Brandt, Phys. Rev. B: Condens. Matter **68**, 054506 (2003); E. H. Brandt, Physica C (Amsterdam) **404**, 74 (2004).
46. A. M. Campbell and J. E. Evetts, Adv. Phys. **50**, 1249 (2001).
47. G. Blatter, M. V. Feigel'man, V. B. Geshkenbein, A. I. Larkin, and V. M. Vinokur, Rev. Mod. Phys. **66**, 1125 (1994).